Conduction electrons in GaAs: Five-level $\mathbf{k}\cdot\mathbf{p}$ theory and polaron effects

P. Pfeffer
Institute of Physics, Polish Academy of Sciences, PL-02-668 Warsaw, Poland

W. Zawadzki*
Institut für Experimentalphysik, Johannes Kepler Universität, A-4040 Linz, Austria
(Received 28 July 1989)

Properties of conduction electrons in GaAs are described theoretically using a five-level $\mathbf{k}\cdot\mathbf{p}$ model, which consistently accounts for inversion asymmetry of the material. The dispersion relation $E(\mathbf{k})$ is computed and it is shown that the conduction band is both nonparabolic and nonspherical. The energy dependence of the electron effective mass, the energy-momentum relation in the forbidden gap, and the spin splitting of the band are calculated. Analytical expressions for the band-edge effective mass, the spin splitting, and the Landé factor g^* are presented, taking explicitly into account an interband matrix element of the spin-orbit interaction. A five-level $\mathbf{P}\cdot\mathbf{p}$ theory for the conduction band in the presence of an external magnetic field is developed. Resonant and nonresonant effects due to polar electron–optic-phonon interaction are included in the theory. The spin g value of conduction electrons is calculated as a function of energy and magnetic field. Spin-doublet splitting of the cyclotron resonance and the cyclotron-resonance-mass anisotropy are described. A comparison of the theory with experimental data of various authors is used to determine important band parameters for GaAs. It is shown that away from the band edge the polaron effects in GaAs are comparable to the band-structure effects.

I. INTRODUCTION

Gallium arsenide has become in recent years the second most important material for semiconductor applications. This has motivated numerous experimental investigations of the three-dimensional and two-dimensional systems involving GaAs. On the other hand, the theoretical band structure of GaAs used in interpretations of the experimental data has been largely oversimplified. It has been commonly assumed that the conduction band of the material is spherical and parabolic. When this assumption proved manifestly insufficient, a simple nonparabolic spherical model has been used. Such a model is provided by a three-level $\mathbf{k}\cdot\mathbf{p}$ description, in which one takes explicitly into account the Γ_6 conduction level and the Γ_8 and Γ_7 valence levels, neglecting all other bands.[1,2] This model successfully describes the conduction bands of narrow-band-gap materials InSb, InAs, and $Hg_{1-x}Cd_xTe$,[3] since in this case the Γ_6-Γ_8 and Γ_6-Γ_7 interactions dominate. The model also has the merit of simplicity, providing analytical expressions for the eigenenergies and eigenfunctions.[3]

However, it has become increasingly clear that the simplest three-level $\mathbf{k}\cdot\mathbf{p}$ model is not sufficient to describe correctly the conduction band of GaAs. Hermann and Weisbuch[4] indicated that it is not possible to account for the band-edge values of the effective mass m_0^* and the Landé factor g_0^* within this framework. Experiments on the electron-spin relaxation showed that the Kramers degeneracy of the conduction band is lifted due to lack of inversion symmetry in the zinc-blende lattice. Cyclotron-resonance data of high magnetic fields demonstrated a pronounced band's nonparabolicity,[5] while the data for different field orientations exhibited an observable band's nonsphericity.[6] All these features cannot be described by the three-level model with neglected distant bands.

A natural extension of the three-level model is the approach of Kane,[1] in which the $\mathbf{k}\cdot\mathbf{p}$ interactions with distant bands are included in the second-order perturbation theory (i.e., up to k^2 terms). A similar approach, taking into account the presence of a magnetic field, is known as the Pidgeon and Brown model[7] (cf. also Grisar *et al.*[8] and Weiler *et al.*[9]). The inclusion of distant bands allows one to describe realistically the Γ_6 conduction band, as well as the Γ_8 and the Γ_7 valence bands in narrow-gap semiconductors. However, as far as the conduction band of GaAs is concerned, this approach has two shortcomings. The first is practical: the model contains quite a few band parameters which do not have a clear physical meaning and which can be determined only by interpreting numerous data, as was the case for InSb.[10] The second is more fundamental: GaAs is not a narrow-band-gap semiconductor and the fundamental gap E_0 between the the Γ_6 and Γ_8 levels is about 1.5 eV, while the gap E_1 between the Γ_6 and the upper Γ_7 conduction level is about 3 eV. Thus, the $\mathbf{k}\cdot\mathbf{p}$ interaction across the gap E_0 is not really dominant and one may not expect even an improved three-level model to work well for GaAs. It has been recently shown that this model gives a weaker band nonparabolicity than the one observed experimentally.[11]

An alternative approach to that of Kane[1] and of Pidgeon and Brown[7] has been proposed by Ogg[12] (cf. also

Refs. 13 and 14). It uses the band-decoupling scheme of Luttinger and Kohn[15] to higher orders of the $\mathbf{k}\cdot\mathbf{p}$ perturbation. This way one obtains an effective one-band Hamiltonian, which accounts for a band's nonparabolicity (up to k^4 terms), nonsphericity, and spin splitting. As demonstrated by Golubev *et al.*,[6] this scheme is useful when discussing anisotropy of the cyclotron-resonance data. Otherwise, however, this formalism neglects higher powers of k terms, it requires a large number of parameters, employs complicated symmetry considerations, and it is inconvenient in finding the corresponding wave functions.

Having in mind a precise description of the conduction band in GaAs and similar materials, we have developed a five-level $\mathbf{k}\cdot\mathbf{p}$ model, which takes explicitly into account two additional conduction levels Γ_8^c and Γ_7^c. A similar approach for the $B=0$ case has been proposed by Rössler.[16] In our description we take consistently into account the lack of inversion symmetry by including the interband spin-orbit term $\bar{\Delta}$ (cf. Ref. 17), and we show that it plays a substantial role in the description of magneto-optical data.

Although GaAs is a weakly polar material, it has been shown recently that some of its magneto-optical properties can be understood only by accounting for polar interaction between electrons and phonons.[18,19] To this end we incorporate into our description nonresonant and resonant polaron effects and demonstrate that indeed they are comparable to the band-structure effects away from the band edge.

II. FIVE-LEVEL $\mathbf{k}\cdot\mathbf{p}$ THEORY

We first consider the case of no external fields. The initial one-electron eigenvalue problem reads

$$\left[\frac{\mathbf{p}^2}{2m_0}+V_0(\mathbf{r})+\frac{\hbar}{4m_0^2c^2}(\sigma\times\nabla V_0)\cdot\mathbf{p}\right]\Psi=E\Psi\ , \quad (1)$$

where V_0 is the periodic lattice potential, m_0 is the free-electron mass, and the spin-orbit term is written in the standard notation. We look for solutions of (1) in the form of Luttinger and Kohn (LK),[15]

$$\Psi_k^m(\mathbf{r})=\exp(i\mathbf{k}\cdot\mathbf{r})\sum_l c_l^m(k)u_l(\mathbf{r})\ . \quad (2)$$

The summation is over all bands and the index m indicates the band of interest. The LK periodic amplitudes satisfy (1) at a band's extremum (at $k=0$ in our case),

$$\left[\frac{\mathbf{p}^2}{2m_0}+V_0(\mathbf{r})+\frac{\hbar}{4m_0^2c^2}(\sigma\times\nabla V_0)\cdot\mathbf{p}\right]u_l=E_{l0}u_l\ , \quad (3)$$

where E_{l0} is the edge energy of the lth band. The LK functions are orthonormal: $(1/\Omega)\langle u_{l'}|u_l\rangle=\delta_{l'l}$, where the integration is over the unit cell Ω. We insert (2) into Eq. (1) and use (3). Multiplying on the left by $(1/\Omega)u_l^*$, and integrating over the unit cell, one obtains

$$\sum_l\left[\left[E^{(l)}+\frac{\hbar^2k^2}{2m_0}-E\right]\delta_{l'l}+\frac{\hbar}{m_0}\mathbf{k}\cdot\mathbf{p}_{l'l}+H_{l'l}^{\text{s.o.}}\right]c_l^m=0\ . \quad (4)$$

The $E^{(l)}$ energies are defined below. The index $l'=1,2,3,\ldots$ runs over the bands, and

$$\mathbf{p}_{l'l}=\frac{1}{\Omega}\left\langle u_{l'}\left|\mathbf{p}+\frac{\hbar}{4m_0c^2}(\sigma\times\nabla V_0)\right|u_l\right\rangle\ . \quad (5)$$

The second term on the right-hand side (rhs) of (5) appears to lead to linear k terms in the energy $E(k)$ and it has been often cited in the literature in this context. However, as shown by Bir and Pikus,[20] this term vanishes for $l=l'$. There exist other sources of linear k terms involving combinations of the spin-orbit and $\mathbf{k}\cdot\mathbf{p}$ interactions (cf. Kane[21]).

If the u_l amplitudes satisfy rigorously Eq. (3), the interband spin-orbit terms $H_{l'l}^{\text{s.o.}}$ do not appear in (4). However, we will use functions which do not satisfy (3) exactly, so that $H_{l'l}^{\text{s.o.}}$ remain.

In the following, we consider a five-level model (5LM) of the band structure at $k=0$ (cf. Fig. 1). The set of LK amplitudes used in our calculations is specified in Table I. Periodic functions S and X,Y,Z,X',Y',Z' are assumed to be real and to transform like s-like and p-like atomic functions under operations of the tetrahedral symmetry group. The X',Y',Z' functions denote the conduction p-type levels; the X,Y,Z functions denote the valence p-type levels. The u_l functions given in Table I diagonalize the spin orbit within (Γ_8^c,Γ_7^c) and (Γ_8^v,Γ_7^v) multiplets. As a consequence, due to inversion asymmetry of the zinc-blende lattice, there exists also a spin-orbit coupling $\bar{\Delta}$ between the above multiplets (Pollak *et al.*[17]). One could choose a more complicated basis, in which the interband spin-orbit term would not appear, but this would in turn complicate the interband matrix elements of the momentum.

In the basis of Table I (taken in order, $u_1,u_9,u_3,u_{11},u_5,u_{13},u_7,u_8,u_2,u_{10},u_4,u_{12},u_6,u_{14}$), the matrix (4) takes the form (6) at right, in which $k_\pm=(k_x\pm ik_y)/\sqrt{2}$ and $\lambda=E-\hbar^2k^2/2m_0$.

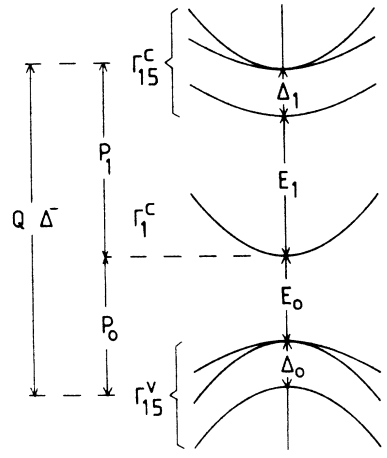

FIG. 1. Five-level model for the conduction band of GaAs near the Γ point of the Brillouin zone. The interband matrix elements of momentum and of the spin-orbit interaction are also indicated.

(6)

$$
\begin{array}{cccccccccccccc}
G_1'-\lambda & 0 & 0 & \sqrt{\frac{1}{3}}P_1k_- & \frac{1}{3}\bar{\Delta} & \sqrt{\frac{1}{3}}Qk_z & 0 & -\sqrt{\frac{2}{3}}P_1k_z & 0 & -\sqrt{\frac{2}{3}}Qk_- & Qk_+ \\
 & G_1'-\lambda & 0 & -P_1k_+ & -\sqrt{\frac{1}{3}}Qk_z & \frac{1}{3}\bar{\Delta} & -\sqrt{\frac{2}{3}}Qk_- & 0 & -\sqrt{\frac{2}{3}}Qk_- & 0 & \sqrt{\frac{1}{3}}Qk_- \\
 & & E_1'-\lambda & \sqrt{\frac{2}{3}}P_1k_- & 0 & \sqrt{\frac{2}{3}}Qk_z & -\frac{2}{3}\bar{\Delta} & \sqrt{\frac{2}{3}}P_1k_z & -Qk_+ & \sqrt{\frac{2}{3}}P_0k_z & 0 & -\sqrt{\frac{1}{3}}P_0k_z \\
 & & & -\lambda & \sqrt{\frac{1}{3}}P_0k_+ & -P_0k_- & \sqrt{\frac{2}{3}}P_0k_+ & 0 & \sqrt{\frac{2}{3}}P_1k_z & 0 & 0 & 0 \\
 & & & & E_0'-\lambda & 0 & 0 & -\sqrt{\frac{2}{3}}P_1k_z & 0 & 0 & 0 & 0 \\
 & & & & & G_0'-\lambda & 0 & 0 & -\sqrt{\frac{1}{3}}Qk_z & 0 & 0 & 0 \\
 & & & & & & G_1'-\lambda & \sqrt{\frac{1}{3}}P_1k_+ & 0 & \sqrt{\frac{1}{3}}Qk_z & \frac{1}{3}\bar{\Delta} & -\sqrt{\frac{2}{3}}Qk_z \\
 & & & & & & & -\lambda & E_1'-\lambda & \sqrt{\frac{2}{3}}Qk_z & -\frac{2}{3}\bar{\Delta} & \sqrt{\frac{2}{3}}P_0k_- \\
 & & & & & & & & E_0'-\lambda & P_0k_+ & 0 & 0 \\
 & & & & & & & & & E_0'-\lambda & 0 & G_0'-\lambda
\end{array}
$$

Due to the appearance of the off-diagonal element $\bar{\Delta}$, the band-edge energies $E^{(l)}$ on the diagonal of (6) are not the observable energies $E_0, E_1, \Delta_0, \Delta_1$ (cf. Fig. 1), but energies which become the observable ones when the matrix is diagonalized at $k=0$. Taking the zero of energy at the Γ_6 edge, one obtains

$$
\begin{aligned}
&E^{(1)}=E^{(2)}=G_1' \ , \\
&E^{(3)}=E_1' \ , \\
&E^{(4)}=0 \ , \\
&E^{(5)}=E^{(6)}=E_0' \ , \\
&E^{(7)}=G_0' \ ,
\end{aligned}
\tag{7}
$$

where

$$
\begin{aligned}
G_1' &= \frac{G_1+E_0}{2}+\left[\left[\frac{G_1-E_0}{2}\right]^2-\frac{\bar{\Delta}^2}{9}\right]^{1/2} , \\
E_0' &= \frac{G_1+E_0}{2}-\left[\left[\frac{G_1-E_0}{2}\right]^2-\frac{\bar{\Delta}^2}{9}\right]^{1/2} , \\
G_0' &= \frac{G_0+E_1}{2}-\left[\left[\frac{G_0-E_1}{2}\right]^2-\frac{4\bar{\Delta}^2}{9}\right]^{1/2} , \\
E_1' &= \frac{G_0+E_1}{2}+\left[\left[\frac{G_0-E_1}{2}\right]^2-\frac{4\bar{\Delta}^2}{9}\right]^{1/2} ,
\end{aligned}
\tag{8}
$$

in which $G_0=E_0+\Delta_0$ and $G_1=E_1+\Delta_1$. In GaAs, $\bar{\Delta}$ is small and the above energies are close to the observable ones.

The spin-orbit energies are defined as

$$
\begin{aligned}
\Delta_0 &= -\frac{3i\hbar}{4m_0^2c^2}\langle X|[\nabla V_0,\mathbf{p}]_y|Z\rangle \ , \\
\Delta_1 &= -\frac{3i\hbar}{4m_0^2c^2}\langle X'|[\nabla V_0,\mathbf{p}]_y|Z'\rangle \ , \\
\bar{\Delta} &= -\frac{3i\hbar}{4m_0^2c^2}\langle X|[\nabla V_0,\mathbf{p}]_y|Z'\rangle \ ,
\end{aligned}
\tag{9}
$$

and the momentum matrix elements are

$$
\begin{aligned}
P_0 &= \frac{-i\hbar}{m_0\Omega}\langle S|p_x|X\rangle \ , \\
P_1 &= \frac{-i\hbar}{m_0\Omega}\langle S|p_x|X'\rangle \ , \\
Q &= \frac{-i\hbar}{m_0\Omega}\langle X|p_y|Z'\rangle = \frac{i\hbar}{m_0\Omega}\langle X'|p_y|Z\rangle \ .
\end{aligned}
\tag{10}
$$

Equating the determinant of the matrix (6) to zero, one can calculate numerically the $E(\mathbf{k})$ dependence resulting from the five-level model if the band-edge energies and the matrix elements are known.

We use the energy gaps measured experimentally. Thus we take $E_0=-1.519$ eV,[22,23] $\Delta_0=-0.341$ eV,[23] $E_1=2.969$ eV,[23,24] and $\Delta_1=0.171$ eV.[23] The sign and value of the interband spin-orbit energy $\bar{\Delta}$ lately has become a subject of interest.[25,26] We take $\bar{\Delta}=-0.061$ eV, calculated with the use of the empirical pseudopotential

TABLE I. Luttinger-Kohn periodic amplitudes used in the five-level model. The total angular momentum j and the band-edge energies $E^{(l)}$ shown in the middle entries refer to functions on both sides.

j_z	u_1	j	$E^{(l)}$	u_1	j_z
$\frac{1}{2}$	$u_1=\sqrt{1/3}R'_+\downarrow-\sqrt{2/3}Z'\uparrow$	$\frac{3}{2}$	G'_1	$u_8=\sqrt{1/3}R'_-\uparrow+\sqrt{2/3}Z'\downarrow$	$-\frac{1}{2}$
$\frac{3}{2}$	$u_2=R'_+\uparrow$	$\frac{3}{2}$	G'_1	$u_9=-R'_-\downarrow$	$-\frac{3}{2}$
$\frac{1}{2}$	$u_3=\sqrt{2/3}R'_+\downarrow+\sqrt{1/3}Z'\uparrow$	$\frac{1}{2}$	E'_1	$u_{10}=\sqrt{2/3}R'_-\uparrow-\sqrt{1/3}Z'\downarrow$	$-\frac{1}{2}$
$\frac{1}{2}$	$u_4=iS\uparrow$	$\frac{1}{2}$	0	$u_{11}=iS\downarrow$	$-\frac{1}{2}$
$\frac{1}{2}$	$u_5=\sqrt{1/3}R_+\downarrow-\sqrt{2/3}Z\uparrow$	$\frac{3}{2}$	E'_0	$u_{12}=\sqrt{1/3}R_-\uparrow+\sqrt{2/3}Z\downarrow$	$-\frac{1}{2}$
$\frac{3}{2}$	$u_6=R_+\uparrow$	$\frac{3}{2}$	E'_0	$u_{13}=-R_-\downarrow$	$-\frac{3}{2}$
$\frac{1}{2}$	$u_7=\sqrt{2/3}R_+\downarrow+\sqrt{1/3}Z\uparrow$	$\frac{1}{2}$	G'_0	$u_{11}=\sqrt{2/3}R_-\uparrow-\sqrt{1/3}Z\downarrow$	$-\frac{1}{2}$

method of Gorczyca.[27]

We use also the band-edge values

$$m_0^*(\text{expt})=0.0660m_0,\quad g_0^*=-0.44$$

determined in the cyclotron resonance[28] and in the spin resonance,[29,30] respectively. We discuss the polaron effects in Sec. V. It should be mentioned, however, that a nonresonant polaron correction must be accounted for when determining the bare electron mass m_0^*. Using the relation $m_0^*(\text{expt})=m_{\text{pol}}^*=m_0^*(1+\alpha/2)/(1+\alpha/3)$ (cf. Ref. 19), and the polar coupling constant $\alpha=0.065$, we calculate the bare mass $m_0^*=0.0653m_0$. This value is used in the $\mathbf{P}\cdot\mathbf{p}$ calculations for electrons in the presence of a magnetic field.

The momentum matrix elements P_0,P_1,Q have been treated as adjustable parameters in the overall best description of various experimental data. This procedure is outlined in the next section.

It has been noticed by Hermann and Weisbuch[4] that also the five-level $\mathbf{k}\cdot\mathbf{p}$ model cannot account for the band-edge values of m_0^* and g_0^*. We follow their procedure by adding the far-band contributions C and C' to m_0^* and g_0^*, respectively. This is equivalent to adding the term $(\hbar^2k^2/2m_0)C$ to the $E(\mathbf{k})$ relation obtained from 5LM. This way of including the far bands is admittedly an approximation. In principle, different far-band contributions should be included in the diagonal terms of the matrix (6). However, since we are interested mainly in the conduction band, the above procedure should give good results.

Thus, our model contains all in all five adjustable parameters. Our best adjusted values for the conduction band of GaAs are

$$E_{P_0}=27.86\text{ eV},\quad E_{P_1}=2.36\text{ eV},\quad E_Q=15.56\text{ eV},$$

in the standard units $E_P=2m_0P^2/\hbar^2$, and

$$C=-2.15\quad\text{and}\quad C'=-0.0215\ .$$

The above value of C has been obtained by taking into account the polaron correction, i.e., doing the $\mathbf{P}\cdot\mathbf{p}$ calculations (for the presence of a magnetic field) with the bare electron mass and including, subsequently, nonresonant and resonant polaron corrections (cf. Sec. V). In the nonmagnetic calculations we have used the experimental mass value $m_0^*(\text{expt})$ and, in order to have the same values of P_0, P_1, and Q, we have used a slightly different value of $C=-2.31$.

It should be noted that, within the framework of 5LM, the linear k terms do not appear.

III. k·p THEORY: RESULTS

We first calculate the $E(\mathbf{k})$ dependence for the conduction band. In the five-level model the conduction band is nonspherical, nonparabolic, and spin split (for a given general direction of $\mathbf{k}$). The nonsphericity is related to the Q terms. The spin splitting is related to all four elements P_0, P_1, Q, and $\bar{\Delta}$ [cf. (14)], but more particularly it is due to nonvanishing values of P_1 and $\bar{\Delta}$ (which vanish in crystals with inversion symmetry). Figure 2 shows the calculated $E(\mathbf{k})$ dependence for the three directions of $\mathbf{k}$.

In order to describe explicitly the band nonparabolicity and to facilitate calculations which do not require high precision, we introduce an effective two-level formula,

$$\frac{\hbar^2k^2}{2m_0^*}=E\left[1+\frac{E}{E_0^*}\right],\tag{11}$$

in which $m_0^*=m_0^*(\text{expt})$ and an effective value of $E_0^*>0$

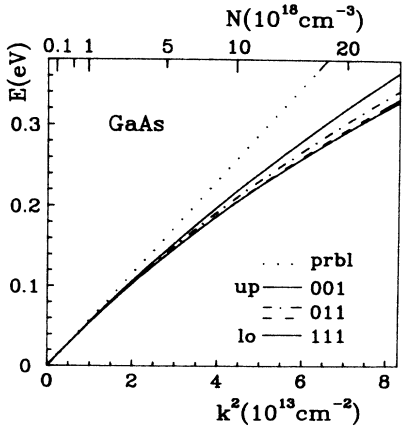

FIG. 2. Dispersion relations $E(\mathbf{k})$ for the conduction band of GaAs. The dotted line indicates parabolic spherical band. The upper solid line shows the dispersion for $\mathbf{k}\|[001]$ according to 5LM, the lower solid line the same for $\mathbf{k}\|[111]$, and the dashed-dotted and dashed lines the dispersions of the spin-up and spin-down states for $\mathbf{k}\|[011]$, respectively.

is adjusted to fit the mean $E(\mathbf{k})$ value at $k=5.5\times10^6$ cm^{-1}, averaged over the three $\mathbf{k}$ directions (values for $\mathbf{k}\|[001]$ and $\mathbf{k}\|[111]$ are counted twice as they are spin degenerate). Equation (11) has been used often in the description of InSb, InAs, and other narrow-band-gap materials and it is easily applicable to various observable properties.[31] Our adjusted value is $E_0^*=0.98$ eV. Comparing the effective value E_0^* with the fundamental gap $|E_0|$, one can see that 5LM describes a considerably stronger nonparabolicity than the two-level model with the real energy gap (a parabolic band corresponds to $E_0^*=\infty$). Equation (11) is more general than it may appear, since it represents the first two terms of the general expansion of $k^2(E)$ in powers of E, cf. Ref. 31. It should be borne in mind, however, that the description (11) is increasingly less valid as k becomes large.

Figure 3 shows the electron velocity: $v_i=\hbar^{-1}\partial E/\partial k_i$ for $\mathbf{k}\|[001]$. The dashed line has been calculated for the two-level formula (11) with $E_0^*=1.52$ eV. In the latter case the velocity reaches the maximum value asymptotically for large energies, which is characteristic of the semirelativistic behavior.[32] In the five-level description the velocity goes through a maximum of $v_{\max}\approx10^8$ cm/sec. Experimentally, the highest electron velocities of $v=9\times10^7$ cm/sec have been reported in experiments with ballistic electrons.[33]

At the band edge the conduction band is spherical and the effective mass can be defined unequivocally. Using the second-order perturbation theory with respect to k terms in the matrix (6), we have derived the following expression for the effective mass at the Γ_6 edge:

$$\frac{m_0}{m_0^*}=1-\frac{1}{3}\left[E_{P_0}\left[\frac{2G_1'}{E_0G_1}+\frac{E_1'}{E_1G_0}\right]+E_{P_1}\left[\frac{2E_0'}{E_0G_1}+\frac{G_0'}{E_1G_0}\right]+\tfrac{4}{3}\bar{\Delta}\sqrt{E_{P_0}\cdot E_{P_1}}\left[\frac{1}{E_1G_0}-\frac{1}{E_0G_1}\right]\right]+C\,, \tag{12}$$

in which the primed quantities have been defined in (8). For $\bar{\Delta}=0$ the above formula reduces to that given by Hermann and Weisbuch.[4]

For a spherical or spheroidal band with an arbitrary nonparabolicity, an effective electron mass may be defined, relating the velocity $\mathbf{v}$ to the pseudomomentum $\hbar\mathbf{k}$.[31] Such a definition does not seem possible for the warped energy band with which we deal. However, one can define a cyclotron-resonance effective mass for a given direction of magnetic field (cf. Sec. VI). For sufficiently low magnetic fields the cyclotron-resonance mass is a quasicontinuous quantity. In particular, in a spherical but nonparabolic band the cyclotron-resonance mass at low fields is equal to the momentum mass: $1/m^*=(1/\hbar^2k)\,dE/dk$, defined by the relation $m^*\mathbf{v}=\hbar\mathbf{k}$.

The details of the calculation of the Landau levels are described below. In Fig. 4 we show the cyclotron-resonance masses calculated at low field intensities for three principal directions of magnetic field. The mass values are compared with experimental results of various authors and various techniques. The data at high Fermi energies are well described by 5LM. In the effective two-band description (11), the energy-dependent effective mass is $m^*(E)=m_0^*(1+2E/E_0^*)$ (cf. Ref. 31).

In Fig. 5 we show a calculated spin splitting of the electron energies in GaAs for the $\mathbf{k}\|[110]$ direction. This splitting is due to the lack of inversion symmetry and obeys the relation $E_\downarrow(\mathbf{k})=E_\uparrow(-\mathbf{k})$. The splitting vanishes at $k=0$ and at the zone edge $k=3\pi/2a_0$. We also show for comparison the results of Christensen and Car-

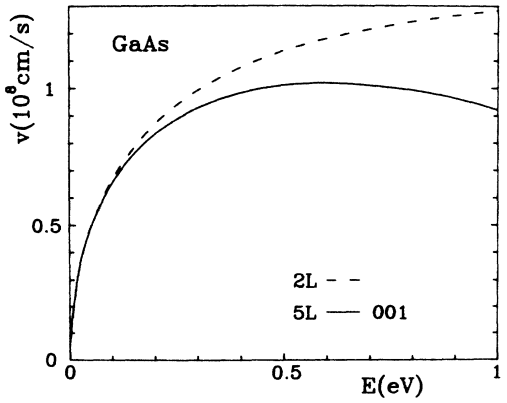

FIG. 3. The electron velocity in the conduction band of GaAs vs the electron energy, as calculated according to the two-level $\mathbf{k}\cdot\mathbf{p}$ model (dashed line) and using 5LM for $\mathbf{k}\|[001]$ (solid line).

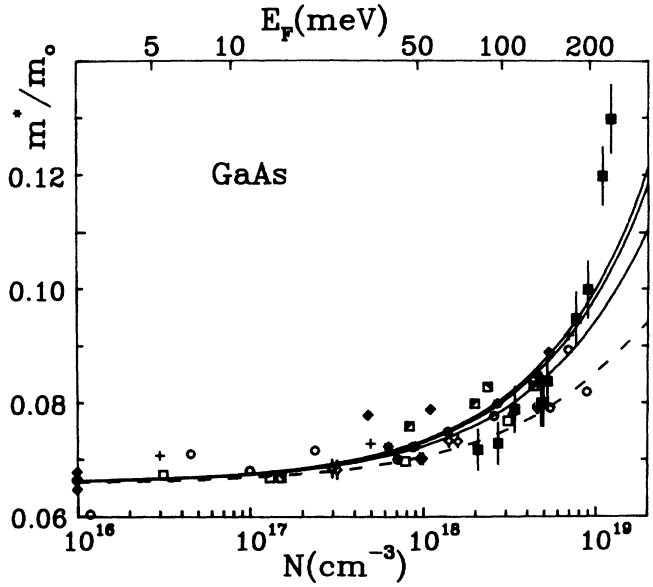

FIG. 4. The cyclotron-resonance effective mass of electrons in GaAs vs the Fermi energy (upper abscissa) and the corresponding free-electron density (lower abscissa). The solid lines show the results of 5LM calculations for three principal directions of the magnetic field. Experimental data: ○, Y. I. Ukhanov (Ref. 34); +, H. Piller (Ref. 35); □, W. M. De Meis (Ref. 36); ◇, A. Raymond *et al.* (Ref. 37); ∗, G. Torkar (Ref. 38); ♦, W. G. Spitzer and J. M. Whelan (Ref. 39); ●, C. G. Olson and D. W. Lynch (Ref. 40); ◩, K. Murase *et al.* (Ref. 41); ◪, M. Cardona (Ref. 42); ■, E. P. Rashevskaya *et al.* (Ref. 43).

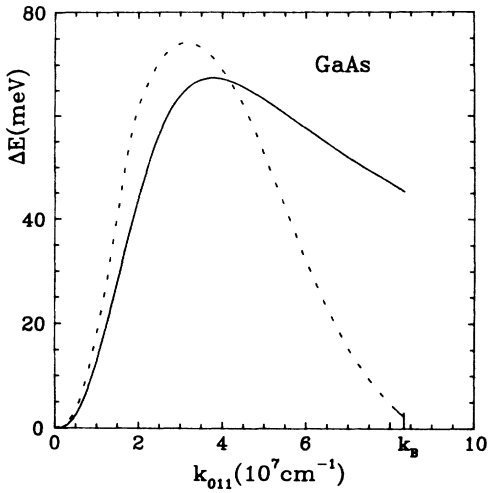

FIG. 5. Spin splitting of the conduction band in GaAs due to inversion asymmetry vs the wave vector $\mathbf{k}\|[011]$, as calculated according to 5LM (solid line). The dashed line shows the results of LMTO calculation.

dona,[44] obtained from a self-consistent linear muffin-tin orbitals (LMTO) calculation (adjusted band model). The comparison shows that our calculation correctly describes the spin splitting up to $k \approx 2.5\times10^7$ cm^{-1} and accounts for its maximum.

At low k values the inversion asymmetry splitting is proportional to k^3. Using matrix (6) and the third-order perturbation theory with respect to k terms we have derived the following expression for the splitting at low k,

$$\Delta E = 2\gamma[k^2(k_x^2k_z^2+k_y^2k_x^2+k_z^2k_y^2)-9k_x^2k_y^2k_z^2] , \quad (13)$$

where

$$\gamma = \frac{4}{3}\frac{Q}{E_0E_1G_0G_1}\left[P_0P_1(E_0'E_1'-G_0'G_1') - \frac{\bar{\Delta}}{3}\left[P_0^2(2G_1'+E_1')-P_1^2(2E_0'+G_0')\right]\right] . \quad (14)$$

For $\bar{\Delta}=0$, expression (14) reduces to the formula published by Zawadzki *et al.*[45] Using our parameters we calculate, for GaAs, $\gamma = 24.12$ eV Å^{-3}.

The value of γ can be measured in experiments on spin relaxation of conduction electrons (Dyakonov and Perel' mechanism[46]). Using this method Aronov *et al.*[47] estimated, for GaAs, $\gamma = 20.9$ eV Å^{-3}. [This has been calculated from the value $\alpha=0.06$, using the relation $2\gamma = \alpha h^3/(2m_0^{*3}/|E_0|)^{1/2}$.] Marushchak *et al.*[48] estimated $\gamma = 24.5$ eV Å^{-3} (from $\alpha=0.07$). Thus our calculation is in good agreement with the experimental data.

In Fig. 6 we show the $E(\mathbf{k})$ relation in the forbidden gap of GaAs, calculated for $\mathbf{k}^2<0$ (i.e., imaginary k values) with the use of 5LM and $\mathbf{k}\|[001]$. The dotted line shows the same for the two-level model (11) with $|E_0| = 1.52$ eV. This region of energies is not accessible classically and the experimental values have been obtained in tunneling experiments on Schottky barriers.[49,50] We get a qualitative agreement between the theory and experiments, but the latter are not precise enough to draw quantitative conclusions.

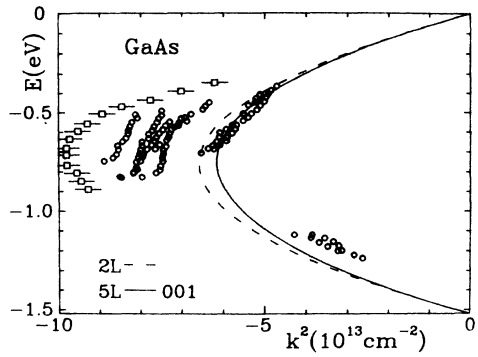

FIG. 6. The dispersion $E(\mathbf{k})$ for imaginary k values in the forbidden gap of GaAs. The dashed line has been calculated according to the two-level model, the solid line according to 5LM for $\mathbf{k}\|[001]$. The experimental data: squares, Padovani and Stratton (Ref. 49); circles, Conley and Mahan (Ref. 50).

Finally in Fig. 7 we show $E(\mathbf{k})$ dependences for the light-hole and split-off valence bands for $\mathbf{k}\|[100]$ and $\mathbf{k}\|[110]$. These have been calculated using 5LM with the above band parameters and $C=0$. The light-hole band is seen to be strongly spin split. In the split-off band the spin splitting is much smaller. The calculated light-hole masses at the band edge are $m_{lh}^*(\mathbf{k}\|[100]) = 0.080\,82m_0$, $m_{lh}^*(\mathbf{k}\|[110]) = 0.070\,54m_0$, and $m_{lh}^*(\mathbf{k}\|[111]) = 0.068\,13m_0$. These are to be compared with experimental values: $m_{lh}^*(\mathbf{B}\|[001]) = 0.087m_0$,[51] $m_{lh}^* = 0.082m_0$,[52] and $m_{lh}^*(\mathbf{B}\|[001]) = 0.082m_0$.[53]

For the split-off band we calculate for the three principal directions of $\mathbf{k}$ approximately the same value $m_{s.o.}^* = 0.1653m_0$. This is to be compared with the measured values of $m_{s.o.}^*(\mathbf{B}\|[001]) = 0.170m_0$,[51] $m_{s.o.}^* = 0.159m_0$,[52] and $m_{s.o.}^* = 0.154m_0$.[54]

Thus 5LM gives a good description of the light-hole and split-off bands, particularly if one would include, in addition, appropriate far-band contributions. The 5LM description considerably modifies results of the three-level model, in which $E(\mathbf{k})$ for the light holes may not go below the energy of $2\Delta_0/3$ (cf. Kane[21]). The $E(\mathbf{k})$ depen-

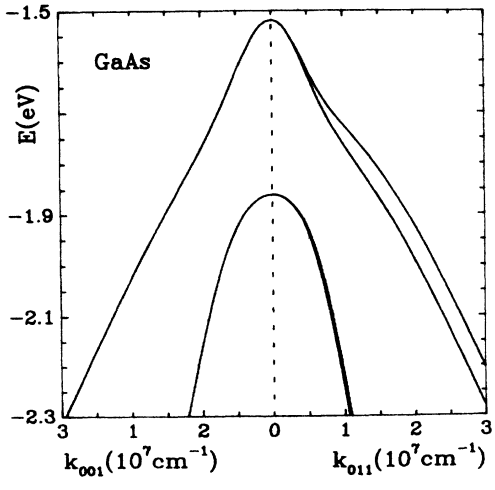

FIG. 7. The dispersion relations $E(\mathbf{k})$ for the light-hole and the split-off valence bands in GaAs, as calculated according to 5LM for two $\mathbf{k}$ directions.

dence shown in Fig. 7 describes the physical reality considerably better.

On the other hand, one may not expect 5LM to describe the heavy-hole band well, since it includes the $\mathbf{k}\cdot\mathbf{p}$ interaction of the Γ_8^v(hh) edge with only one multiplet (Γ_8^c,Γ_7^c). This is not enough to reproduce correctly the heavy-hole masses.

IV. P·p THEORY

A. Five-level model for $B\neq0$

Precise values of band parameters near a band's extremum may be obtained from magneto-optical experiments and their comparison with the theory. It is therefore of interest to describe the conduction band of GaAs-like materials in the presence of an external magnetic field. Below, we develop the five-level model near the Γ point for the case $B\neq0$.

The initial one-electron eigenvalue problem reads

$$\left[\frac{1}{2m_0}\mathbf{P}^2+V_0(\mathbf{r})+\frac{\hbar}{4m_0^2c^2}(\boldsymbol{\sigma}\times\nabla V_0)\cdot\mathbf{P}+\mu_B\mathbf{B}\cdot\boldsymbol{\sigma}\right]\Psi=E\Psi\,, \tag{15}$$

where $\mathbf{P}=\mathbf{p}+e\,\mathbf{A}$ is the kinetic momentum, $\mathbf{A}$ is the vector potential of magnetic field $\mathbf{B}$, and the Pauli term is written in the standard notation. Due to the presence of a magnetic field the eigenvalue problem (15) is not periodic. We look for its solutions in the form

$$\Psi=\sum_l f_l(\mathbf{r})u_l(\mathbf{r})\,, \tag{16}$$

in which $u_l(\mathbf{r})$ are the Luttinger-Kohn periodic functions satisfying (3), and $f_l(\mathbf{r})$ are the envelope functions, slowly varying within the unit cell. The summation is over all energy bands. Inserting (16) into (15), using (3), multiplying on the left by $(1/\Omega)u_{l'}^*$, and integrating over the unit cell, one obtains[55]

$$\left[\left[\frac{1}{2m_0}P^2+E^{(l)}-E\right]\delta_{l'l}+\frac{1}{m_0}\mathbf{p}_{l'l}\cdot\mathbf{P}+\mu_B\mathbf{B}\cdot\boldsymbol{\sigma}_{l'l}+H_{l'l}^{\text{s.o.}}\right]f_l=0\,. \tag{17}$$

The matrix elements $\mathbf{p}_{l'l}$ are defined in (5), and $\boldsymbol{\sigma}_{l'l}=(1/\Omega)\langle u_{l'}|\boldsymbol{\sigma}|u_l\rangle$. The interband matrix elements of the spin-orbit interaction have been retained for the reasons discussed in Sec. II.

Equation (17) represents a set of coupled differential equations for the envelope functions f_l. It involves as yet no approximations, apart from the requirement of slow variation of $\mathbf{A}(\mathbf{r})$ and $f_l(\mathbf{r})$ within the unit cell. We proceed as in the no-field case specifying 5LM (shown in Fig. 1) and taking the set of basis of LK functions given in Table I. The resulting eigenvalue problem is written in matrix form (17), in which the matrix is given in Eq. (18) at right.

$$\left(\begin{array}{cccccccccccccc}
G_1'+\frac{\mu}{3}-\lambda & 0 & -(\sqrt{8}/3)\mu & \frac{1}{\sqrt{3}}P_1'P_- & & & & & & & -\sqrt{2/3}P_1'P_z & & & \\
 & G_1'-\mu-\lambda & 0 & -P_1'P_+ & & A_1 & & & 0 & & 0 & & D & \\
 & & E_1'-\frac{\mu}{3}-\lambda & \sqrt{2/3}P_1'P_- & & & & & & & 1/\sqrt{3}P_1'P_z & & & \\
 & & & -\mu-\lambda & 1/\sqrt{3}P_0'P_+ & -P_0'P_- & \sqrt{2/3}P_0'P_+ & \sqrt{2/3}P_1'P_z & 0 & -1/\sqrt{3}P_1'P_z & 0 & \sqrt{2/3}P_0'P_z & 0 & -1/\sqrt{3}P_0''P_z \\
 & & & & E_0'+\frac{\mu}{3}-\lambda & 0 & -(\sqrt{8}/3)\mu & & & & -\sqrt{2/3}P_0'P_z & & & \\
 & & & & & E_0'-\mu-\lambda & 0 & & -D & & 0 & & 0 & \\
 & & & & & & G_0'-\frac{\mu}{3}-\lambda & & & & 1/\sqrt{3}P_0'P_z & & & \\
 & & & & & & & G_1'-\frac{\mu}{3}-\lambda & 0 & (\sqrt{8}/3)\mu & 1/\sqrt{3}P_1'P_+ & & & \\
 & & & & & & & & G_1'+\mu-\lambda & 0 & P_1'P_- & & A_z & \\
 & & & & & & & & & E_1'+\frac{\mu}{3}-\lambda & \sqrt{2/3}P_1'P_+ & & & \\
 & & & & & & & & & & \mu-\lambda & 1/\sqrt{3}P_0'P_- & P_0'P_+ & \sqrt{2/3}P_0'P \\
 & & & & & & & & & & & E_0'-\frac{\mu}{3}-\lambda & 0 & (\sqrt{8}/3)\mu \\
 & & & & & & & & & & & & E_0'+\mu-\lambda & 0 \\
 & & & & & & & & & & & & & G_0'+\frac{\mu}{3}-\lambda
\end{array}\right) \tag{18}$$

The same ordering as in (6) has been used. We define $P_0'=P_0/\hbar$, $P_1'=P_1/\hbar$, $Q'=Q'/\hbar$, $\lambda=E-P^2/2m_0$, $\mu=\mu_B B$, and $P_\pm=(P_x\pm iP_y)/\sqrt{2}$. The ordering has been chosen in such a way that for $Q'=0$ and $P_z=0$ the matrix (18) factorizes into two 7×7 sets. The matrices A_1, A_2, and D are given below for principal directions of magnetic field. The direction of **B** is specified by the vector potential **A**. When specifying **A** one should keep in mind that the functions u_l used to obtain the matrix (18) are written in the coordinate system parallel to [100], [010], and [001] crystal directions.

B. Approximation $Q=0$

We first consider the approximation $Q=0$, which results in a spherical conduction band. Consequently, the energies do not depend on the direction of magnetic field. We take the gauge $\mathbf{A}=(-By,0,0)$, corresponding to $\mathbf{B}\|[001]$. One can then look for the envelope functions in the form $f_l=\exp(ik_x x+ik_z z)\phi_l(y)$. We further simplify the problem by considering the case $k_z=0$, which is of main interest in magneto-optical and magnetotransport phenomena.

For $Q=0$ and $k_z=0$ the set (17) factorizes into two 7×7 sets, which are soluble in terms of harmonic-oscillator functions. The first set has the solutions

$$\Psi_N^-=\begin{cases}C_1|n-1\rangle\\ C_9|n+1\rangle\\ C_3|n-1\rangle\\ C_{11}|n\rangle\\ C_5|n-1\rangle\\ C_{13}|n+1\rangle\\ C_7|n-1\rangle\end{cases}, \tag{19}$$

where $N=n$, and $|n\rangle=\exp(ik_x x)\phi_n[(y-y_0)/L]$, in which $y_0=k_x L^2$ is the center of oscillations, $L=(\hbar/eB)^{1/2}$ is the magnetic radius, and ϕ_n are the harmonic-oscillator functions. The C_l coefficients in front of oscillator functions with negative indices are equal to zero. The corresponding number matrix is calculated from (18) performing the operations

$$P_+|n\rangle=-(\hbar/L)(n+1)^{1/2}|n+1\rangle\ , \tag{20}$$

$$P_-|n\rangle=-(\hbar/L)n^{1/2}|n-1\rangle\ , \tag{21}$$

$$P^2|n\rangle=2(\hbar/L)^2(n+\tfrac{1}{2})|n\rangle\ . \tag{22}$$

This way one obtains Eq. (23), at right, in which $P_0''=P_0/L$ and $P_1''=P_1/L$. The eigenvalues give the magnetic energies of the seven bands involved ("b" or "$-$" states) for the $Q=0$ (spherical) case.

For the second set the eigenfunctions are

$$\begin{pmatrix}
G_1'+\frac{\mu}{3}+2\mu(n-1+\frac{1}{2})-E & 0 & -\sqrt{8}\mu/3 & -P_1''\sqrt{n/3} & \bar{\Delta}/3 & 0 & -P_0''\sqrt{n/3} & 0\\
0 & G_1'-\mu+2\mu(n+1+\frac{1}{2})-E & 0 & P_1''\sqrt{n+1} & 0 & \bar{\Delta}/3 & 0 & -P_0''\sqrt{n+1}\\
-\sqrt{8}\mu/3 & 0 & E_1'-\frac{\mu}{3}+2\mu(n-1+\frac{1}{2})-E & -P_1''\sqrt{(2/3)n} & 0 & 0 & -P_0''\sqrt{(2/3)n} & 0\\
-P_1''\sqrt{n/3} & P_1''\sqrt{n+1} & -P_1''\sqrt{(2/3)n} & 0-\mu+2\mu(n+\frac{1}{2})-E & 0 & 0 & 0 & -\sqrt{8}\mu/3\\
\bar{\Delta}/3 & 0 & 0 & 0 & E_0'+\frac{\mu}{3}+2\mu(n-1+\frac{1}{2})-E & 0 & 0 & 0\\
0 & \bar{\Delta}/3 & 0 & 0 & 0 & E_0'-\mu+2\mu(n+1+\frac{1}{2})-E & 0 & 0\\
-P_0''\sqrt{n/3} & P_0''\sqrt{n+1} & -P_0''\sqrt{(2/3)n} & 0 & 0 & 0 & G_0'+\frac{\mu}{3}+2\mu(n-1+\frac{1}{2})-E & 0\\
0 & 0 & 0 & -\sqrt{8}\mu/3 & 0 & 0 & 0 & G_0'-\frac{\mu}{3}+2\mu(n-1+\frac{1}{2})-E
\end{pmatrix} \tag{23}$$

$$\Psi_N^+ = \begin{cases} C_8|n+1\rangle \\ C_2|n-1\rangle \\ C_{10}|n+1\rangle \\ C_4|n\rangle \\ C_{12}|n+1\rangle \\ C_6|n-1\rangle \\ C_{14}|n+1\rangle \end{cases} . \tag{24}$$

The corresponding number matrix is calculated from (18) performing operations indicated in (20)–(22). The result is Eq. (25), at right. The eigenvalues give the magnetic energies of the seven bands involved ("a" or "+" states) for the $Q=0$ (spherical) case.

$$\begin{array}{|ccccccc|} \hline
G_1'-\frac{\mu}{3}+2\mu(n+1+\frac{1}{2})-E & 0 & \sqrt{8}\mu/3 & -P_1''\sqrt{(n+1)/3} & \bar{\Delta}/3 & 0 & 0 \\
0 & G_1'+\mu+2\mu(n-1+\frac{1}{2})-E & 0 & -P_1''\sqrt{n} & 0 & \bar{\Delta}/3 & 0 \\
\sqrt{8}\mu/3 & 0 & E_1'+\frac{\mu}{3}+2\mu(n+1+\frac{1}{2})-E & -P_1''\sqrt{(2/3)(n+1)} & 0 & 0 & -2\bar{\Delta}/3 \\
-P_1''\sqrt{(n+1)/3} & -P_1''\sqrt{n} & -P_1''\sqrt{(2/3)(n+1)} & 0+\mu+2\mu(n+\frac{1}{2})-E & -P_0''\sqrt{(n+1)/3} & -P_0''\sqrt{n} & -P_0''\sqrt{(2/3)(n+1)} \\
\bar{\Delta}/3 & 0 & 0 & -P_0''\sqrt{(n+1)/3} & E_0'-\frac{\mu}{3}+2\mu(n+1+\frac{1}{2})-E & 0 & \sqrt{8}\mu/3 \\
0 & \bar{\Delta}/3 & 0 & -P_0''\sqrt{n} & 0 & E_0'+\mu+2\mu(n-1+\frac{1}{2})-E & 0 \\
0 & 0 & -2\bar{\Delta}/3 & -P_0''\sqrt{(2/3)(n+1)} & \sqrt{8}\mu/3 & 0 & G_0'+\frac{\mu}{3}+2\mu(n+1+\frac{1}{2})-E \\ \hline
\end{array} \tag{25}$$

Using (23) and (25) it is possible to derive an analytical expression for the spin g value at the edge of the conduction band (which does not involve the Q terms). Calculating the polynomial $F_a(E_a,n,B)=0$ from (25) and the polynomial $F_b(E_b,n,B)=0$ from (23), one can calculate $(dE_a/dB)_{B=0}$ and $(dE_b/dB)_{B=0}$, which determine the linear expansion of the energies in B. Their difference gives the band-edge g value in the five-level model. The result is

$$g_0^* = 2+\frac{2}{3}\left[-E_{P_0}\left(\frac{E_1'}{E_1G_0}-\frac{G_1'}{E_0G_1}\right)+E_{P_1}\left(\frac{E_0'}{E_0G_1}-\frac{G_0'}{E_1G_0}\right)-\tfrac{2}{3}\bar{\Delta}\sqrt{E_{P_0}\cdot E_{P_1}}\left(\frac{2}{E_1G_0}+\frac{1}{E_0G_1}\right)\right]+2C' , \tag{26}$$

in which the constant C' represents the far-band contribution. For $\bar{\Delta}=0$, the above formula reduces to the expression given by Hermann and Weisbuch.[4] We have used (12) together with (26) for the band-edge electron mass in a preliminary fitting of the band parameters.

C. General case: B||[001]

We now turn to the general case of $Q\neq 0$, in which energies depend on the direction of the magnetic field. We consider first **B**||[001] crystal direction, taking $\mathbf{A}=(-By,0,0)$. The matrices A_1, A_2, and D, indicated in (18) are then obtained in the form

$$A_1 = \begin{bmatrix} \frac{1}{3}\bar{\Delta} & \frac{1}{\sqrt{3}}Q'P_z & 0 \\ -\frac{1}{\sqrt{3}}Q'P_z & \frac{1}{3}\bar{\Delta} & -\sqrt{2/3}Q'P_z \\ 0 & \sqrt{2/3}Q'P_z & -\frac{2}{3}\bar{\Delta} \end{bmatrix} , \tag{27}$$

$$A_2=\begin{bmatrix} \frac{1}{3}\bar{\Delta} & \frac{1}{\sqrt{3}}Q'P_z & 0 \\ -\frac{1}{\sqrt{3}}Q'P_z & \frac{1}{3}\bar{\Delta} & -\sqrt{2/3}Q'P_z \\ 0 & \sqrt{2/3}Q'P_z & -\frac{2}{3}\bar{\Delta} \end{bmatrix}, \quad (28)$$

$$D=\begin{bmatrix} 0 & -\sqrt{2/3}Q'P_- & Q'P_+ \\ -\sqrt{2/3}Q'P_- & 0 & \sqrt{1/3}Q'P_- \\ -QP_+ & \sqrt{1/3}Q'P_- & 0 \end{bmatrix}. \quad (29)$$

In order to find the eigenenergies we use the method of Evtuhov,[56] applied for the first time to warped valence bands of Ge. The method is based on the fact that deviations from a band's sphericity are small. Thus we look for each envelope function of the set in the form

$$f_l(r)=\exp(ik_z z)\sum_m c_m^l |m\rangle , \quad (30)$$

where $|m\rangle$ functions have been defined above and c_m^l are numerical coefficients. We again set $k_z=0$. To focus the reader's attention we consider the first equation of (18). The forms (30) are introduced to this equation and indicated operations performed according to (20)–(22). Next, the equation is multiplied on the left by $\langle 0|$ and integrated over the crystal volume. This leaves only a few nonvanishing terms and the result is a simple algebraic equation for a few c_m^l. Next, the same equation is multiplied by $\langle 1|$ and integrated, resulting in the next algebraic equation for a few c_m^l. The procedure is repeated with higher oscillator functions. A similar calculation is then carried out with the remaining 13 equations of the set (18). This way one obtains an infinite set of equations for c_m^l. The solutions of this set contain magnetic energies for all the bands involved and all the quantum numbers N.

In practice, one solves the problem by truncating the infinite set and looking for good approximate solutions. For this purpose one should order the equations for c_m^l according to increasing quantum number N. This is best done by requiring that for $Q=0$ the infinite matrix factorizes into the 7×7 matrices (23) and (25), ordered according to increasing $N^{\pm}$: 0^+, 0^-, 1^+, 1^-, etc. When this is done one finds that the infinite matrix (with Q terms) factorizes into two independent infinite matrices. The latter, when truncated to the "nearest neighbors" coupled by the Q matrices, have the following schematic forms:

$$\begin{bmatrix} N'-3,+ & Q & 0 \\ & N,- & Q \\ & & N+1,+ \end{bmatrix} \quad (31)$$

for the N^- states (set b), and

$$\begin{bmatrix} N-1,- & Q & 0 \\ & N,+ & Q \\ & & N+3,- \end{bmatrix} \quad (32)$$

for the N^+ states (set a). Here N^+ and N^- denote matrices (23) and (25), respectively, and Q symbolically denotes matrices containing only Q terms.

If one is interested in energies of $N^{\pm}$ states for not overly high numbers N, it is enough to include the nearest-neighbor matrices and to truncate the rest. This is good enough for the Γ_6 conduction band since the Q terms do not couple directly to the Γ_6 band edge. We have checked that for low N an inclusion of the second-neighbor matrices changes magnetic energies in the conduction band only by a fraction of a percent. Thus for $\mathbf{B}\|[100]$ the calculation amounts to a diagonalization of a 21×21 matrix.

D. General case: B‖[110]

For the $\mathbf{B}\|[110]$ crystal direction we take the gauge $\mathbf{A}=(B/2)(0,x,-x)$. In order to obtain the spherical part of the matrix in the previous form, we define a coordinate system with the new z' axis parallel to [011] direction:

$$x'=(y-z)/\sqrt{2},\quad y'=-x,\quad z'=(y+z)/\sqrt{2}\ . \quad (33)$$

Next, the new basis of the periodic functions $u_l'(r')$ is defined to have the new functions in the new coordinates in the same form, as given in Table I. For instance, $u_2'=(X'+iY')\uparrow'$. This is achieved by transforming X',Y',Z' from X,Y,Z according to (33) and the spin functions according to (cf. Kane[1])

$$\begin{bmatrix} \uparrow' \\ \downarrow' \end{bmatrix}=\begin{bmatrix} e^{-i\phi/2}\cos(\frac{1}{2}\theta) & e^{i\phi/2}\sin(\frac{1}{2}\theta) \\ -e^{-i\phi/2}\sin(\frac{1}{2}\theta) & e^{i\phi/2}\cos(\frac{1}{2}\theta) \end{bmatrix}\begin{bmatrix} \uparrow \\ \downarrow \end{bmatrix}, \quad (34)$$

where $\phi=90°$ and $\theta=45°$. Next, the matrix elements of the $\mathbf{p}\cdot\mathbf{P}$ operator are calculated using the new basis $u_l'(r)$, expressed in the old components $X,Y,Z,\uparrow,\downarrow$. This gives the $\mathbf{p}\cdot\mathbf{P}$ matrix in terms of three operators: $(P_y-P_z)/\sqrt{2}\pm iP_y$ and $(P_y+P_z)/\sqrt{2}$. Upon introducing the new coordinates (33) the vector potential is first transformed as a vector $\mathbf{A}'(\mathbf{r})$ in the new system and then expressed in the new coordinates. This gives $\mathbf{A}'(\mathbf{r}')=(-By',0,0)$. Transforming the momentum operators into the new coordinates, one finds that the above operators define exactly raising, lowering, and parallel operators for the magnetic problem in these coordinates: $P'=(P_x'+iP_y')/\sqrt{2}$ and P_z', respectively. This completes the calculation of the eigenvalue problem for $\mathbf{B}\|[011]$.

The spherical part of the matrix (18) (without Q terms) is the same as for the $\mathbf{B}\|[001]$ case, while A_1, A_2, and D take the form

$$A_1=\begin{bmatrix} \frac{Q'(P_+-P_-)}{2\sqrt{2}}+\frac{\bar{\Delta}}{3} & \frac{Q'(3P_++P_-)}{2\sqrt{6}} & \frac{Q'(P_--P_+)}{2} \\ \frac{-Q'(3P_-+P_+)}{2\sqrt{6}} & \frac{Q'(P_--P_+)}{2\sqrt{2}}+\frac{\bar{\Delta}}{3} & \frac{-Q'(3P_-+P_+)}{2\sqrt{3}} \\ \frac{Q'(P_--P_+)}{2} & \frac{Q'(3P_++P_-)}{2\sqrt{3}} & -\frac{2\bar{\Delta}}{3} \end{bmatrix}, \tag{35}$$

$$A_2=\begin{bmatrix} \frac{Q'(P_+-P_-)}{2\sqrt{2}}+\frac{\bar{\Delta}}{3} & \frac{Q'(3P_-+P_+)}{2\sqrt{6}} & \frac{Q'(P_--P_+)}{2} \\ -\frac{Q'(3P_++P_-)}{2\sqrt{6}} & \frac{Q'(P_--P_+)}{2\sqrt{2}}+\frac{\bar{\Delta}}{3} & \frac{-Q'(3P_++P_-)}{2\sqrt{3}} \\ \frac{Q'(P_--P_+)}{2} & \frac{Q'(3P_-+P_+)}{2\sqrt{3}} & -\frac{2\bar{\Delta}}{3} \end{bmatrix}, \tag{36}$$

$$D=\begin{bmatrix} 0 & \frac{Q'P_z}{\sqrt{3}} & -\frac{Q'P_z}{\sqrt{2}} \\ \frac{Q'P_z}{\sqrt{3}} & 0 & -\frac{Q'P_z}{\sqrt{6}} \\ \frac{Q'P_z}{\sqrt{2}} & -\frac{Q'P_z}{\sqrt{6}} & 0 \end{bmatrix}. \tag{37}$$

It is seen that for $k_z=0$ there is $D=0$, so that for this case the matrix (18) factorizes in general into two 7×7 matrices for "a" and "b" states.

Using Evtuhov's procedure one obtains two number matrices, which have the following schematic form (identical for both spin states)

$$\begin{bmatrix} N-3,\pm & 0 & Q & 0 & 0 \\ & N-1,\pm & Q & 0 & 0 \\ & & N,\pm & Q & Q \\ & & & N+1,\pm & 0 \\ & & & & N+3,\pm \end{bmatrix}. \tag{38}$$

The matrices on the diagonal are defined in (23) and (25), while Q denotes matrices involving Q terms [in general, different from those in (31) and (32)]. Again, when considering energies of not too high $N^{\pm}$ states it is enough to include the first neighboring matrices coupled directly by Q matrices to the state in question. This requires a numerical diagonalization of a 35×35 matrix, as illustrated by (38).

E. General case: B||[111]

Finally, we consider the case of the B||[111] crystal direction. The gauge is $\mathbf{A}=B[(x-y)/2,(x-y)/2,(y-x)]$, the transformation rules become

$$\begin{aligned} x'&=(x+y-2z)\sqrt{6}\,, \\ y'&=(y-x)/\sqrt{2}\,, \\ z'&=(x+y+z)/\sqrt{3}\,, \end{aligned} \tag{39}$$

and the spins transform according to (3), where $\phi=45°$ and $\theta=54.73°$. Again, we require that in the rotated system the periodic functions have the same form as Table I. This allows one to find their form in terms of X,Y,Z and $\uparrow,\downarrow$ functions. The $\mathbf{p}\cdot\mathbf{P}$ operator is then calculated using this basis. This gives the matrix expressed in terms of three operators: $[P_x+P_y-2P_z\pm i\sqrt{3}(P_y-P_x)]/\sqrt{12}$ and $(P_x+P_y+P_z)/\sqrt{3}$. In the rotated coordinate system the vector potential becomes $\mathbf{A}'(\mathbf{r}')=(-By',0,0)$, while the above operators become $P'_{\pm}=(P'_x\pm iP'_y)/\sqrt{2}$ and P'_z, respectively. This completes the derivation of the eigenvalue problem for the B||[111] direction. Again the spherical part of the matrix is the same as for the B||[001] and B||[011] directions, while the Q terms are different,

$$A_1=\begin{bmatrix} -i\frac{1}{\sqrt{3}}Q'P_z+\frac{\bar{\Delta}}{3} & -i\frac{2}{3}Q'P_+ & i\sqrt{2/3}Q'P_z \\ -i\frac{2}{3}Q'P_- & i\frac{1}{\sqrt{3}}Q'P_z+\frac{\bar{\Delta}}{3} & -i\frac{\sqrt{8}}{3}Q'P_- \\ i\sqrt{2/3}Q'P_z & -i\frac{\sqrt{8}}{3}Q'P_+ & -\frac{2}{3}\bar{\Delta} \end{bmatrix}, \tag{40}$$

$$A_2=\begin{bmatrix} -i\frac{1}{\sqrt{3}}Q'P_z+\frac{\bar{\Delta}}{3} & i\frac{2}{3}Q'P_- & i\sqrt{2/3}Q'P_z \\ i\frac{2}{3}Q'P_+ & i\frac{1}{\sqrt{3}}Q'P_z+\frac{\bar{\Delta}}{3} & i\frac{\sqrt{8}}{3}Q'P_+ \\ i\sqrt{2/3}Q'P_z & i\frac{\sqrt{8}}{3}Q'P_- & -\frac{2}{3}\bar{\Delta} \end{bmatrix}, \tag{41}$$

$$D=\begin{bmatrix} 0 & -i\frac{\sqrt{2}}{3}Q'P_+ & -i\frac{1}{\sqrt{3}}Q'P_- \\ -i\frac{\sqrt{2}}{3}Q'P_+ & 0 & i\frac{1}{3}Q'P_+ \\ i\frac{1}{\sqrt{3}}QP_- & i\frac{1}{3}Q'P_+ & 0 \end{bmatrix} . \tag{42}$$

Using Evtuhov's procedure one obtains a number matrix, which factorizes into two independent matrices. Truncating the problem for N^+ and N^- states to the nearest-neighbor interaction via the Q terms, one has to diagonalize numerically the following matrices (schematically). For the N^- (set b) states

$$\begin{bmatrix} N-3,- & Q & 0 & 0 \\ & N,- & Q & Q \\ & & N-1,+ & 0 \\ & & & N+3,- \end{bmatrix} . \tag{43}$$

For the N^+ (set a) states,

$$\begin{bmatrix} N-3,+ & 0 & Q & 0 \\ & N+1,- & Q & 0 \\ & & N,+ & Q \\ & & & N+3,+ \end{bmatrix} . \tag{44}$$

The diagonal matrices are defined in (23) and (25), while Q denotes matrices involving only Q terms. Thus for the $\mathbf{B}\|[111]$ direction and $k_z=0$ a calculation of magnetic energies requires numerical diagonalization of 28×28 matrices.

As mentioned above, the truncation of the infinite matrix into blocks coupled directly by Q matrices to the state of interest, $N^{\pm}$, provides a very good approximation for not overly high quantum numbers N. However, since the matrix elements of the lowering and raising operators behave roughly as $\sqrt{N}$ and the energy differences stay approximately the same, the first-neighbor coupling becomes progressively worse as N gets higher.

V. MAGNETOPOLARON EFFECTS

It has been recognized during the last few years that resonant and nonresonant polaron effects in GaAs are comparable to band-structure effects.[5,18,19] Clearly, some properties are more affected by the electron-phonon interaction than others, but, in principle, polarons should be included in any precise description of magneto-optical phenomena in this material. Below we describe the main features of our approach. Since we are concerned with magnetic fields below 20 T, i.e., below the resonance condition $\hbar\omega_c\approx\hbar\omega_L$ (where $\hbar\omega_L$ is the energy of the longitudinal-optical phonon), there is no need to employ the Green-function formalism (cf. Ref. 57).

The polar interaction of electrons with longitudinal-optical phonons is introduced in the standard way,[58]

$$H_{Fr}=A\frac{1}{q}(b_q e^{i\mathbf{q}\cdot\mathbf{r}}-b_q^{\dagger}e^{-i\mathbf{q}\cdot\mathbf{r}}) , \tag{45}$$

where $A^2=2\pi e^2\hbar\omega_L(1/\kappa_\infty-1/\kappa_0)$, and κ_∞ and κ_0 are the high-frequency and static dielectric constants, respectively. We are interested in corrections to Landau energies caused by virtual-phonon emission at low energies. Since GaAs is a weakly polar material, the Frölich interaction is treated in the second-order improved Wigner-Brillouin (IBW) perturbation theory.

The perturbed energy of the nth Landau level is given by $E_n=E_n^0+\Delta E_n$, where the correction is

$$\Delta E_n=\sum_{m=0}^{\infty}\sum_{q}\frac{|M_{nm}(q)|^2}{D_{nm}} . \tag{46}$$

M_{nm} are the matrix elements of the Frölich interaction calculated using the Landau wave functions, while the energy denominators are

$$D_{nm}^{IWB}=E_n-(E_m^0+\delta_m+\hbar\omega_L) . \tag{47}$$

The shifts δ_m are related to the improvement of the perturbation theory and they require some consideration.

One proves in the diagrammatic analysis of the polaron problem that in the self-energy calculation—that is, in (46) and (47)—the energies $E_0,E_1,\ldots$ should be final electron energies, i.e., they should already include corrections due to the electron-phonon interaction. On the other hand, it is known that a finite order of the WB perturbation theory (46) is not invariant with respect to the choice of zero of the unperturbed Hamiltonian.[59] Shifting the zero by δ leads to a shift δ of E_n^0 energies in denominators (47) and, in principle, the results should be minimized with respect to this shift. In order to improve the WB perturbation theory according to the above principles, Lassnig in Ref. 18 proposed to take δ_m the same for all levels and equal to $\delta_m=\Delta E_0^{RS}$, where $\Delta E_0^{RS}(B)$ denotes the polaron shift of the zeroth level, calculated using the Rayleigh-Schrödinger (RS) perturbation theory. This choice has the following merits. (1) In calculating ΔE_1 according to (46) the decisive (resonant) term is taken correctly with the final energy $E_0^0+\Delta E_0^{RS}$. (2) At $B=0$ the polaron shift of all levels, calculated with the improved BW theory, is $\Delta E_n=-\alpha\hbar\omega_L$. (3) The polaron energy for the zeroth Landau level at all B is the same for IBW and RS theories. (4) At high fields the lower polaron branch pins to $E_1=E_0+\hbar\omega_L$, which is observed experimentally (cf. Ref. 19). In the following we adopt the ansatz $\delta_n=\Delta E_0^{RS}$.

For the zeroth Landau level all denominators (47) in the sum (46) are nonresonant. The matrix elements of the Frölich interaction between Landau states are well known,[60] and one can express the series (46) by an integral.[61] For the first Landau level one term in (46) can become resonant (the interaction with the zeroth state due to the phonon emission). For this reason we break the sum into $\Delta E^1=\Delta E^1_{nr}+\Delta E^1_{res}$, in which the nonresonant part contains the summation from 1 to ∞ and it is again converted into an integral.[57] The resonant part can be expressed in the form first given by Nakayama,[62]

$$\Delta E^1_{res}=\frac{-\alpha\hbar\omega_L}{\sqrt{L}}\int_0^{\infty}\frac{\exp(-x^2)x^2}{\xi(x+\xi)}dx , \tag{48}$$

where $\xi^2=(E_0^0+\hbar\omega_L+E_0^{RS}-E_1)/\hbar\omega_c$, and α is the polar coupling constant. We have independently calculated the polaron corrections to the spin-up and spin-down Landau levels since the phonon-induced spin-flip interactions are negligible. The values $\alpha=0.065$ (Refs. 18 and 19) and $\hbar\omega_L=36.2$ meV (Refs. 19 and 63) have been used.

At $B=0$ the nonresonant IBW theory gives for all Landau levels $m^*_{pol}=m_0^*(1+\alpha/2)/(1+\alpha/3)$ (cf. Ref. 19). Thus at the beginning we calculate the bare mass m_0^* from the band-edge experimental mass $m^*_{pol}=m_0^*(\text{expt})$. The value of m_0^* is used in the "bare" **P·p** theory and then the polaron effects are introduced. This brings the theoretical band-edge mass at $B=0$ to the observed value $m_0^*(\text{expt})$. However, the resonant polaron contribution becomes important for $n=1$ as B increases, so that the above procedure is nontrivial. When calculating the nonresonant part, involving a summation over the infinite number of levels, we use a parabolic approximation to the energies, i.e., we assume that all levels are equally spaced. In this procedure, however, the value of $\hbar\omega_c$ is computed for each magnetic field from **P·p** theory. In the resonant term (48) the realistic, nonparabolic energies are used.

VI. P·p THEORY: RESULTS

It is now possible to discuss the calculation of the effective masses, shown in Fig. 4. Having computed the Landau energies for a given field orientation, we define a cyclotron-resonance effective mass m^* by the formula $E(N+1,\pm)-E(N\pm)=\hbar eB/m^*$. Such a mass depends in general on the spin orientation, the intensity and direction of the magnetic field, as well as on N. However, it turns out that for low field intensities one obtains the same mass value for a given average electron energy, regardless of whether the energy is reached by changing the spin, N, or B, where the average energy is defined as $E=[E(N+1,\pm)+E(N,\pm)]/2$. This fact allows us to plot the cyclotron-resonance effective masses as functions of energy for various field directions, as shown in Fig. 4.

A similar procedure can be used to calculate the effective Landé factor g^* as a function of energy for various field directions. The g value is defined by the relation $E(N,+)-E(N,-)=g^*\mu_B B$. Again, one obtains the same values of $g^*(E)$ at low magnetic fields regardless of whether the average energy, $E=[E(N,+)-E(N,-)]/2$, is reached by changing N or B. The results for the principal field directions are shown in Fig. 8. They illustrate the common tendency of the g factors in III-V compounds to reach the free-electron value of $+2$ at high electron energies. Since the band-edge value of g^* in GaAs is negative, it crosses zero at achievable electron energies. A similar phenomenon occurs in InSb and InAs.[64]

In Fig. 9 we show calculated g^* factors for $N=1$ and 2 as functions of magnetic field intensity for the principal field directions. It can be seen that for $B>30$ T the g values for $N=0$ and 1 have different signs. This situation was recently realized in pulsed-field experiments of Najda *et al.*[65]

Unequal g values for the $N=0$ and 1 Landau levels result in different energies of the cyclotron resonance (CR) for spin-up ($0^+\rightarrow 1^+$) and spin-down ($0^-\rightarrow 1^-$) transitions.[28,45] In experiments with a fixed light frequency and swept magnetic field one observes a spin doublet of CR, in which the higher-energy transition occurs at a lower field. In high-quality GaAs the spin-doublet is relatively easy to observe since, due to small electron g values, both ground spin states are populated at low temperatures and high magnetic fields. The splitting can be measured to a high accuracy because it is recorded in one sweep of the field, so that it does not require a precise absolute calibration of the magnet. The spin-doublet splitting of CR has been used by Zawadzki *et al.*[45] in the first demonstration that the five-level **P·p** model is necessary for an adequate description of the conduction band in GaAs. The same effect has been used by Golubev *et al.*[6] in the first experimental demonstration that the conduction band in GaAs is nonspherical.

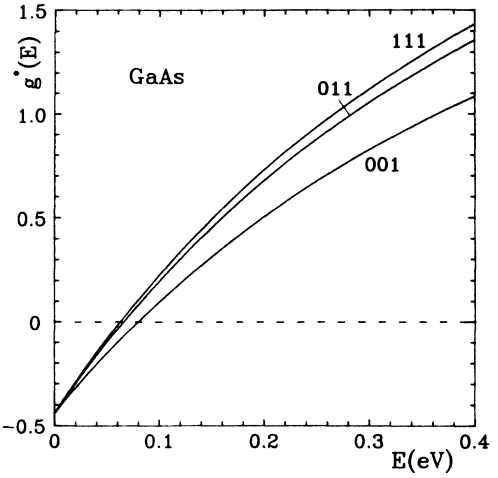

FIG. 8. The Landé factor of conduction electrons in GaAs vs the electron energy, calculated for three directions of magnetic field with the use of 5LM.

In Fig. 10 we show experimental results on the spin-doublet splitting of CR for the three principal field directions, compared to our theoretical description. The splittings ΔB between two CR peaks are plotted as functions

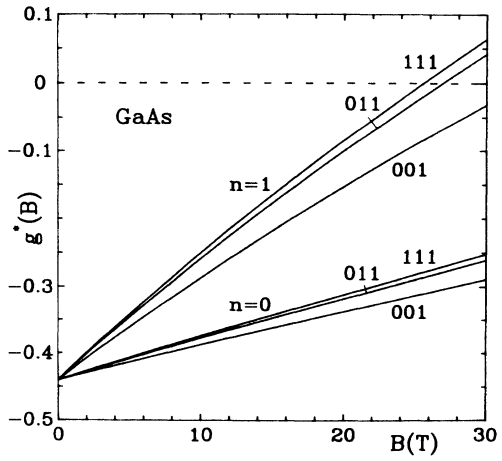

FIG. 9. The Landé factor of conduction electrons in GaAs for the two lowest Landau levels vs magnetic field intensity, calculated for three field directions with the use of 5LM.

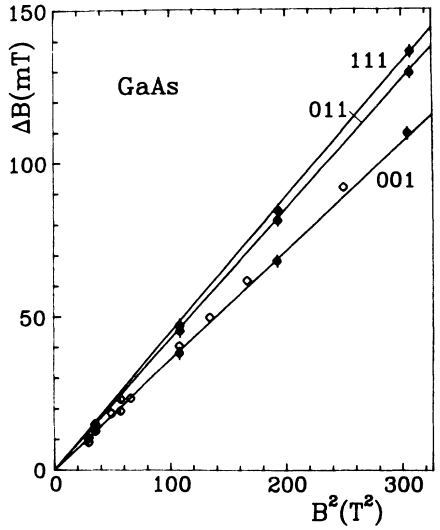

FIG. 10. Spin-doublet splittings of the cyclotron resonance for the conduction electrons in GaAs vs B^2 for three field directions. The solid lines are calculated using 5LM and including polaron effects. Experimental data: half-open circles, Golubev *et al.* (Ref. 6); solid circles, Sigg *et al.* (Ref. 25); open circles, Hopkins *et al.* (Ref. 28).

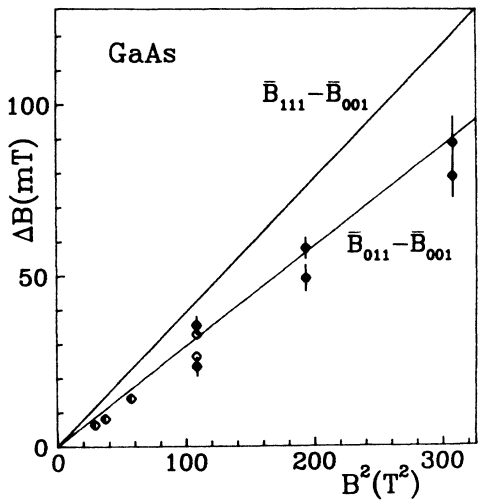

FIG. 11. Shifts of mean cyclotron-resonance field for the conduction electrons in GaAs vs B^2 for different field orientations. The solid lines are calculated using 5LM and including polaron effects. Experimental data: half-open circles, Golubev *et al.* (Ref. 6); solid circles, Sigg *et al.* (Ref. 25); open circles, Hopkins *et al.* (Ref. 28).

of the average resonance field intensity (squared). The thoeretical fit to the anisotropy of the splittings is our main test in determining the parameter Q. As we have mentioned above, Q is responsible for the band nonsphericity within the five-level model. As argued in Ref. 45, the spin-doublet splitting is relatively insensitive to the polaron effects. The reason is that, while both CR energies are substantially affected by the polaron shifts (cf. Fig. 12), the latter are nearly the same for both spin transitions, so that their difference is only weakly affected. It should be emphasized, however, that in contrast to Refs. 25 and 45 the polaron effects have been included in the present description.

In Fig. 11 we show differences of average CR fields measured for different **B** directions, $B_{[111]}-B_{[001]}$ and $B_{[011]}-B_{[001]}$, as functions of magnetic field intensity (squared). These shifts are directly related to the anisotropy of the electron mass. The theoretical shifts are somewhat smaller than the observed ones, i.e., the experimental anisotropy is smaller than the theoretical one. We have been unable to obtain a better fit with parameter values which would describe other experiments well. However, in contrast to the results shown in Fig. 11, the experimental anisotropy observed in GaAs by means of CR at megagauss fields is higher than the theoretical one, calculated for the same band parameters. The discrepancy between the lower-field and higher-field results is not understood at present.

Finally, in Fig. 12 we show the cyclotron-resonance effective masses for the spin-down and spin-up CR transitions versus the resonant energy, as measured and calculated for **B**||[001]. The dashed lines indicate the results of calculation in which the polaron effects are omitted and the theoretical mass at the band edge is taken to be equal to the measured (i.e., polaron) mass. The dashed lines are almost straight. This follows from the fact that, as already mentioned above, in a band described by relation (11), the energy dependence of the momentum mass is $m^*(E)=m_0^*(1+2E/E_0^*)$, i.e., the mass increases linearly with the energy.[31] The solid lines have been calculated including the nonresonant and resonant polaron effects, beginning with the "bare" mass. It can be seen that the resonant polaron effects become increasingly important as the excitation energy approaches the optical-phonon energy. Figure 12 illustrates our previous state-

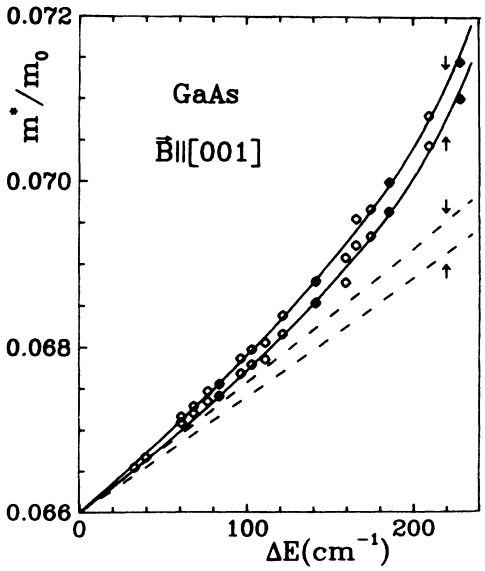

FIG. 12. Cyclotron masses of electrons in GaAs vs transition energy (spin-up and spin-down transitions) for **B**||[001]. Dashed lines: five-level **P**·**p** theory with the band-edge mass equal to the observed value. Solid lines: five-level **P**·**p** theory including resonant and nonresonant polaron contributions. Experimental data: solid circles, Sigg *et al.* (Ref. 25); open circles, Hopkins *et al.* (Ref. 28).

ment that the polaron effects in GaAs are comparable to the band-structure effects.

VII. DISCUSSION

The presented description of conduction electrons in GaAs accounts quite well for a variety of magneto-optical data. The largest discrepancy between theory and experiment, concerning the anisotropy of the cyclotron mass, is shown in Fig. 11. It should be mentioned, however, that at very high magnetic fields of 100 T the same theory gives a mass anisotropy lower than the experimental one,[65] whereas in Fig. 11 the theoretical anisotropy is higher than the experimental one. The best overall fit allowed us to determine important band parameters.

The adjusted best value of the matrix elements P_1 depends strongly on the value of interband spin-orbit energy $\bar{\Delta}$ used in the calculations. In the present analysis we have used $\bar{\Delta}=-0.061$ eV, calculated by the empirical pseudopotential method.[27] Using three different methods, Cardona *et al.*[26] calculated $\bar{\Delta}=-0.11$ eV (LMTO), -0.085 eV [linear combination of atomic orbitals (LCAO)], and -0.07 eV ($\mathbf{k}\cdot\mathbf{p}$). In the five-level $\mathbf{k}\cdot\mathbf{p}$ model of Rössler[16] and in the effective Hamiltonian expansions of Ogg[12] and of Braun and Rössler[14] the existence of $\bar{\Delta}$ has been ignored.

Carrying the self-consistent relativistic LMTO calculation, Christensen and Cardona[44] calculated the spin splitting of the conduction band due to inversion asymmetry. For small k values [cf. our Eq. (13)], they obtained $\gamma=82$ eV Å^3 for an unadjusted band structure, and $\gamma=17$ eV Å^3 for an adjusted band structure. The last value agrees reasonably well with our result of $\gamma=24.12$ eV Å^{-3}.

In a recent paper, Cardona *et al.*[66] also derived formulas for the inversion asymmetry splitting and the g value of conduction electrons in GaAs-type materials using a six-level $\mathbf{k}\cdot\mathbf{p}$ model and taking into account the existence of $\bar{\Delta}$. Their formulas ignore the differences between the energies on the diagonal of the $\mathbf{k}\cdot\mathbf{p}$ matrix and the measured band-edge energies [resulting from the existence of $\bar{\Delta}$; cf. our Eqs. (8)]. There exist additional differences between their formulas and our formulas, but the discrepancies do not affect strongly the numerical values.

ACKNOWLEDGMENTS

One of us (W.Z.) would like to thank Professor Helmut Heinrich for his generous hospitality during his stay in Linz. This work has been partially supported by the Fonds zur Förderung der wissenschaftlichen Forschung in Österreich (Wien, Austria).

*Permanent address: Institute of Physics, Polish Academy of Sciences, PL-02-668 Warsaw, Poland.

[1]E. O. Kane, J. Phys. Chem. Solids **1**, 249 (1957).

[2]R. Bowers and Y. Yafet, Phys. Rev. **115**, 1165 (1959).

[3]W. Zawadzki, in *New Developments in Semiconductors,* edited by P. R. Wallace *et al.* (Noordhoff, Leyden, 1973), p. 441.

[4]C. Hermann and C. Weisbuch, Phys. Rev. B **15**, 823 (1977).

[5]H. Sigg, H. J. A. Bluyssen, and P. Wyder, Solid State Commun. **48**, 897 (1983).

[6]V. G. Golubev, V. I. Ivanov-Omskii, I. G. Minervin, A. V. Osutin, and D. G. Polyakov, Pis'ma Zh. Eksp. Teor. Fiz. **40**, 143 (1984) [JETP. Lett. **40**, 896 (1984)].

[7]C. R. Pidgeon and R. N. Brown, Phys. Rev. **146**, 575 (1966).

[8]R. Grisar, H. Wachering, G. Bauer, J. Wlasak, J. Kowalski, and W. Zawadzki, Phys. Rev. B **18**, 4355 (1978).

[9]M. H. Weiler, R. L. Aggarwal, and B. Lax, Phys. Rev. B **17**, 3269 (1978).

[10]C. L. Littler, D. G. Seiler, R. Kaplan, and R. J. Wagner, Phys. Rev. B **27**, 7473 (1983).

[11]W. Trzeciakowski and D. Wasik, Phys. Rev. B **37**, 8939 (1988).

[12]N. R. Ogg, Proc. Phys. Soc. London **89**, 43 (1966).

[13]H. J. Zeiger and G. W. Pratt, *Magnetic Interactions in Solids* (Oxford University Press, London, 1973).

[14]M. Braun and U. Rössler, J. Phys. C **18**, 3365 (1985).

[15]J. M. Luttinger and W. Kohn, Phys. Rev. **97**, 869 (1955).

[16]U. Rössler, Solid State Commun. **49**, 943 (1984).

[17]F. H. Pollak, C. W. Higginbotham, and M. Cardona, J. Phys. Soc. Jpn. Suppl. **21**, 20 (1966).

[18]G. Lindemann, R. Lassnig, W. Seidenbusch, and E. Gornik, Phys. Rev. B **28**, 4693 (1983).

[19]P. Pfeffer and W. Zawadzki, Solid State Commun. **57**, 847 (1986); Phys. Rev. B **37**, 2695 (1988).

[20]G. L. Bir and G. E. Pikus, *Symmetry and Strain-Induced Effects in Semiconductors* (Wiley, New York, 1974), p. 200.

[21]E. O. Kane, in *Narrow Gap Semiconductors, Physics and Applications,* Vol. 133 of *Lecture Notes in Physics,* edited by W. Zawadzki (Sprnger, Berlin, 1980), p. 13.

[22]D. D. Sell, Phys. Rev. B **6**, 3750 (1972).

[23]D. E. Aspnes and A. A. Studna, Phys. Rev. B **7**, 4605 (1973).

[24]T. C. Chiang, J. A. Knapp, M. Aano, and D. E. Eastman, Phys. Rev. B **21**, 3513 (1980).

[25]H. Sigg. J. A. A. J. Perenboom, P. Pfeffer, and W. Zawadzki, Solid State Commun. **61**, 685 (1987).

[26]M. Cardona, N. E. Christensen, and G. Fasol, in *Proceedings of the 18th International Conference on the Physics of Semiconductors,* edited by O. Engström (World Scientific, Singapore, 1987), p. 1133.

[27]I. Gorczyca (unpublished).

[28]M. A. Hopkins, R. J. Nicholas, P. Pfeffer, W. Zawadzki, D. Gauthier, J. C. Portal, and M. A. Di Forte-Poisson, Semicond. Sci. Technol. **2**, 568 (1987).

[29]A. M. White, I. Hinchcliffe, P. J. Dean, and P. D. Green, Solid State Commun. **10**, 497 (1972).

[30]C. Weisbuch and C. Hermann, Phys. Rev. B **15**, 816 (1977).

[31]W. Zawadzki, Adv. Phys. **23**, 435 (1974).

[32]W. Zawadzki, in *Optical Properties of Solids,* edited by E. D. Haidemenakis (Gordon and Breach, New York, 1970), p. 179.

[33]L. F. Eastman, in *Festkörperprobleme (Advances in Solid State Physics),* edited by P. Grosse (Pergamon/Vieweg, Braunschweig, 1982), Vol. 22, p. 173.

[34]Y. I. Ukhanov, Fiz. Tverd. Tela (Leningrad) **5**, 108 (1963) [Sov. Phys.—Solid State **5**, 75 (1963)].

[35]H. Piller, J. Phys. Soc. Jpn. Suppl. **21**, 206 (1966).

[36]W. M. De Meis, Ph.D. thesis, Harvard University, 1965.
[37]A. Raymond, J. L. Robert, and C. Bernard, J. Phys. C **12**, 2289 (1979).
[38]G. Torkar, Ph.D. thesis, Universität München, 1980.
[39]W. G. Spitzer and J. M. Whelan, Phys. Rev. **114**, 59 (1959).
[40]C. G. Olson and D. W. Lynch, Phys. Rev. **177**, A1231 (1969).
[41]K. Murase, S. Katayama, Y. Ando, and H. Kawamura, Phys. Rev. Lett. **32**, 1481 (1974).
[42]M. Cardona, Phys. Rev. **121**, 752 (1961).
[43]E. P. Rashevskaya, V. I. Fistul, and M. G. Mil'vidskii, Fiz. Tverd. Tela (Leningrad) **8**, 3135 (1966) [Sov. Phys.—Solid State **8**, 2515 (1966)].
[44]N. E. Christensen and M. Cardona, Solid State Commun. **51**, 491 (1984).
[45]W. Zawadzki, P. Pfeffer, and H. Sigg, Solid State Commun. **53**, 777 (1985).
[46]H. I. Dyakonov and V. I. Perel', Fiz. Tverd. Tela (Leningrad) **13**, 3581 (1971) [Sov. Phys.—Solid State **13**, 3023 (1972)].
[47]A. G. Aronov, G. E. Pikus, and A. N. Titkov, Zh. Eksp. Teor. Fiz. **84**, 1170 (1983) [Sov. Phys.—JETP **57**, 680 (1983)].
[48]V. A. Marushchak, M. N. Stepanova, and A. N. Titkov, Fiz. Tverd. Tela (Leningrad) **25**, 3537 (1983) [Sov. Phys.—Solid State **25**, 2035 (1983).
[49]F. A. Padovani and R. Stratton, Phys. Rev. Lett. **16**, 1202 (1966).
[50]J. W. Conley and G. D. Mahan, Phys. Rev. **161**, 681 (1967).
[51]A. L. Mears and R. A. Stradling, J. Phys. C **4**, L22 (1971).
[52]Q. H. F. Vrehen, J. Phys. Chem. Solids **29**, 129 (1968).
[53]M. S. Skolnick *et al.*, J. Phys. C **9**, 2809 (1976).
[54]M. Reine, R. L. Aggarwal, B. Lax, and C. M. Wolfe, Phys. Rev. B **2**, 458 (1970).
[55]W. Zawadzki, in *Narrow Gap Semiconductors, Physics and Applications,* edited by W. Zawadzki (Springer, Berlin, 1980), p. 85.
[56]V. Evtuhov, Phys. Rev. **125**, 1869 (1962).
[57]L. Swierkowski and W. Zawadzki, J. Phys. Soc. Jpn. **49**, Suppl. A, 767 (1980).
[58]G. D. Mahan, *Many Particle Physics* (Plenum, New York, 1980), p. 489.
[59]E. Feenberg, Ann. Phys. (N.Y.) **3**, 292 (1958); R. C. Young, C. I. Biederharn, and E. Feenberg, Phys. Rev. **106**, 1151 (1957).
[60]V. L. Gurevich and Yu. A. Firsov, Zh. Eksp. Teor. Fiz. **47**, 739 (1965) [Sov. Phys.—JETP **20**, 489 (1966)]; F. G. Bass and I. B. Levinson, *ibid.* **49**, 914 (1965) [**22**, 635 (1966)].
[61]D. M. Larsen, Phys. Rev. **142**, 428 (1966).
[62]M. Nakayama, J. Phys. Soc. Jpn. **27**, 636 (1969).
[63]V. Rohrer, Ph.D. thesis, University of Munich, 1982 (unpublished).
[64]W. Zawadzki, Phys. Lett. **4**, 190 (1963).
[65]S. P. Najda, S. Takeyama, N. Miura, P. Pfeffer, and W. Zawadzki, in *Proceedings of the 19th International Conference on the Physics of Semiconductors,* edited by W. Zawadzki (Institute of Physics, Polish Academy of Sciences, Warsaw, 1988), p. 909.
[66]M. Cardona, N. E. Christensen, and G. Fasol, Phys. Rev. B **38**, 1806 (1988).